ADVANCED MATERIALS

Communications

Self-Assembled Nanocomposite Polymer Light-Emitting Diodes with Improved Efficiency and Luminance**

By *Valery Bliznyuk*, *Beat Ruhstaller*, *Phil J. Brock*, *Ulli Scherf*, and *Sue A. Carter**

Hybrid organic and nanoparticle-based systems have been recently studied as prospective materials for optoelectronics applications because they combine the advantages of organic polymers with those of inorganic clusters. For photonic applications, nanoparticles enable a wider variation of the dielectric constant (refractive index) and charge transport properties than polymers.[1] The mesoscale character of nanoparticle dimensions, corresponding to the wavelength of visible light, allows for the assembly of superlattice structures with possible optical band gap properties[2] or with microcavity effects for polymer lasing.[3] Highly efficient photovoltaics can be made through organic dye sensitization of TiO_2 and related nanoparticles.[4,5] More recently, dielectric oxide nanoparticles have been shown to modify the charge transport in polymer light-emitting diodes, resulting in an increase in both the current density and light emission.[6] In this paper, we show that nanoparticles assembled at a semiconducting polymer/electrode interface can also affect charge injection into polymer light-emitting diodes. For the case of negatively charged dielectric SiO_2 monolayers assembled at the anode interface, external electroluminescence quantum efficiencies approaching theoretical limits for radiative singlet decay can be achieved. Moreover, nanoparticle monolayers result in enhanced luminances at lower drive voltages, similar to what has been achieved with conducting polymer layers. These results indicate that interfacial nanoparticle layers offer a general method for enhancing the local electric field across the polymer/anode interface, providing versatility for improving performance of polymer optoelectronic devices.

Since the discovery of electroluminescence in polymers,[7] charge transport and injection in semiconducting polymers has been actively studied with the goal of achieving bright and highly efficient polymer light-emitting diodes operating at low electric fields. A key requirement for high electroluminescent efficiencies is balanced injection of holes and electrons at the anode and cathode interfaces, respectively. Such balance can be dramatically affected by controlling injection through modification of the interface between the semiconducting polymer and the electrodes. Although both electrode surfaces can be modified in principle, the modification of the indium tin oxide (ITO) anode is more common due to the atmospheric stability of the ITO surface that enables "wet" preparation stages (cleaning, chemical modification, and spinning) before the vacuum stages such as evaporation of a metal cathode and protective coatings. For materials limited by hole-injection, the device efficiency can be improved by inserting a hole transporting layer that enables smaller tunneling barriers, or Ohmic injection, from the anode into the highest occupied molecular orbital (HOMO) of the polymer.[8–11] For electron-limited materials, the quantum efficiency can be improved by inserting a layer that effectively blocks electrons from reaching the anode.[12]

In this work, modification of the ITO transparent anode was achieved using self-assembled monolayers and electrostatically assembled SiO_2 nanoparticles. This modification was performed in two stages. First, the 3-aminopropyltriethoxysilane molecules were attached to the ITO surface via chemo-adsorption from an ethanol solution. This procedure is similar to modification of Si described before,[13] allowing NH_3^+ functionalization of the ITO surface. The thickness of a self-assembled organic layer was estimated to be 0.9 nm from atomic force microscopy (AFM) measurements.[13] In the second step of modification, nanoparticles were attached to the surface of ITO via electrostatic physical adsorption from water solution. Adjustment of the pH conditions on the surface of the SAM resulted in protonation of NH_2 groups to NH_3^+ charged groups and the formation of a complete monolayer of negatively charged nanoparticles consisting of SiO_2 (Nissan Chemicals Co., 20 nm diameter) or polystyrene latexes spheres (Interfacial Dynamics Corp., 30 nm diameter) as demonstrated by AFM. The amine functionality also enables attachment of metallic gold nanoparticles (BBI International Co., 40 nm) through chemical tethering to the surface. For comparison, devices were made with bare ITO surfaces cleaned in H_2O/isopropanol bath and with polyaniline-PSS (PAni) conducting polymer layer. Table 1 describes the device structures, electrode modificaton and acronyms contained in the figures.

The semiconducting polymers used in these study were poly(2-methoxy-5-(2′-ethyl-hexoxy)-*p*-phenylene vinylene)

[*] Prof. S. A. Carter, Dr. V. Bliznyuk, Dr. B. Ruhstaller
Physics Department, University of California
Santa Cruz, CA 95064 (USA)
Dr. P. J. Brock
IBM Almaden Research Center
San Jose, CA 95120-6099 (USA)
Dr. U. Scherf
Max Planck Institute for Polymer Research
D-55021 Mainz (Germany)

[**] This work was supported by an NSF Goali Grant DMR#9704177 and the NSF MRSEC Center for Polymer Interface and Macromolecular Assembly.

  0935-9648/99/1510-1257 $ 17.50+.50/0

Table 1. Polymer light-emitting diode device structures and acronyms: Ca is calcium cathode, ITO is indium tin oxide anode, polymer is MEH-PPV or Me-LPPP, SA is self-assembled.

	Device Structure	Notation
1.	Ca 25nm / Polymer 100nm / ITO 150nm	none
2.	Ca 25nm / Polymer 100nm / PAni 100nm / ITO 150nm	PAni
3.	Ca / Polymer / ITO — NH_2-terminated SA monolayer (0.9nm)	NH2
4.	Ca / Polymer / ITO — Nanoparticles monolayer (20-50 nm)	SiO2
5.	Ca / Polymer / ITO — Thermally evaporated SiO layer (20 nm)	SiO
6.	The same as 1, 2, or 4 with Polymer/SiO_2 nanoparticles blend (20% of SiO_2) as an active polymer layer	- " - / Blend

(MEH-PPV: λ_{max} = 596 nm) and the methyl substituted ladder-type poly(*p*-phenylene) (Me-LPPP: λ_{max} = 460 nm), both of which have been well characterized in previous studies.[14,15] Their electroluminescence spectra, shown in Figure 1, reveal the normal vibrational structure. Device performance was also tested with MEH-PPV/SiO_2 nanoparticle blends and nonblended materials to demonstrate compatibility with composite structures. The devices were assembled inside a nitrogen glove box using spinning and thermal evaporated Ca contacts with Al protection layers, as described previously.[16] The Ca electrode provides a nearly Ohmic contact to both MEH-PPV and Me-LPPP. The device areas were 3 mm^2 and the active polymer layer was varied between 40 nm and 800 nm; an optimal thickness of 100 nm ± 10 nm was chosen for the studies presented here. Measurements of *I–V* curves and light output of the devices were made with Keithley 2400 digital amper–volt meter and Keithley 485 picoampmeter operated with LabView software. A spectrometer and calibrated integrating sphere, collecting the forward externally emitted light, were used to measure the electroluminescence spectra and derive the luminances and external quantum efficiencies.

Theoretical quantum efficiencies for polymer electroluminescence materials are difficult to calculate due to uncer-

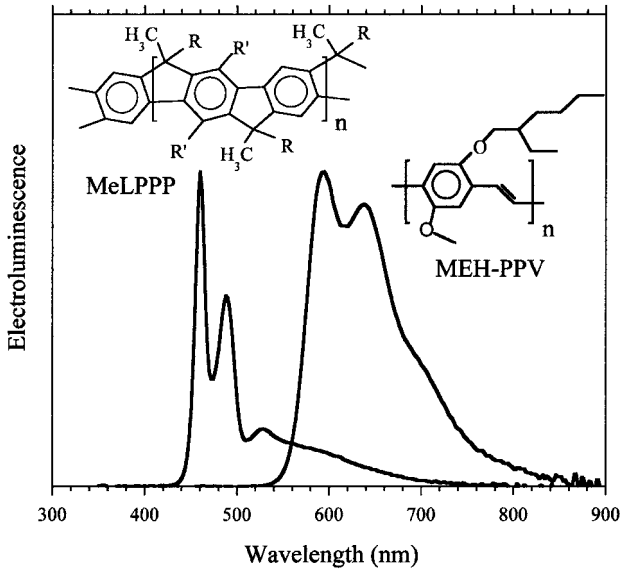

Fig. 1. Electroluminescence spectra for MEH-PPV and Me-LPPP. Inset are the chemical structures of the two materials.

tainty in the nature of the radiative state and the population of singlet versus triplet excited states. Nonetheless, for purposes of comparison we will consider that only the singlet states recombine to emit light, that a negligible amount of light is absorbed by the materials due to a large Stokes shift, and that 25 % of the excited states are singlets. This yields a formula for the external quantum efficiency, η_{ext}, of

$$\eta = 1/4 C b \Phi_{PL} \quad (1)$$

where *C* is the outcoupling efficiency, *b* is the fraction of injected carriers that recombine, and Φ_{PL} is the photoluminescence efficiency.[17,18] For a common planar geometry with preferential alignment of polymer chains along the substrate, the outcoupling efficiency *C* can be approximated by $1/n^2$ (*n*, being the refractive index of glass). If all the factors in Equation 1 are optimized (C = 0.43 and b = 1) the maximum quantum efficiency of MEH-PPV devices is estimated as 2.5 ± 0.5 % since Φ_{PL} is reported to be 20–30 % in thin films.[18] The same parameter will be below 2.0 % for Me-LPPP devices since tendency for chain aggregation and excimer formation reduces Φ_{PL} to below 20 %.[14]

Figure 2a shows measured external quantum efficiency versus applied power for MEH-PPV based devices. Typically, the external quantum efficiencies saturate at high powers to values near 1 %. All the devices prepared with PAni have higher quantum efficiencies than non-modified substrates due to an increase in the work function which results in nearly Ohmic hole injection.[16] The best performance corresponds to PAni/blend and SiO_2/blend devices, and we achieve quantum efficiencies near the theoretical limit of 2.5 % for MEH-PPV devices using the SiO_2 nanoparticle monolayers. This maximum quantum efficiency is reached for PAni based samples only in the limit of low

  0935-9648/99/1510-1258 $ 17.50+.50/0

ADVANCED MATERIALS

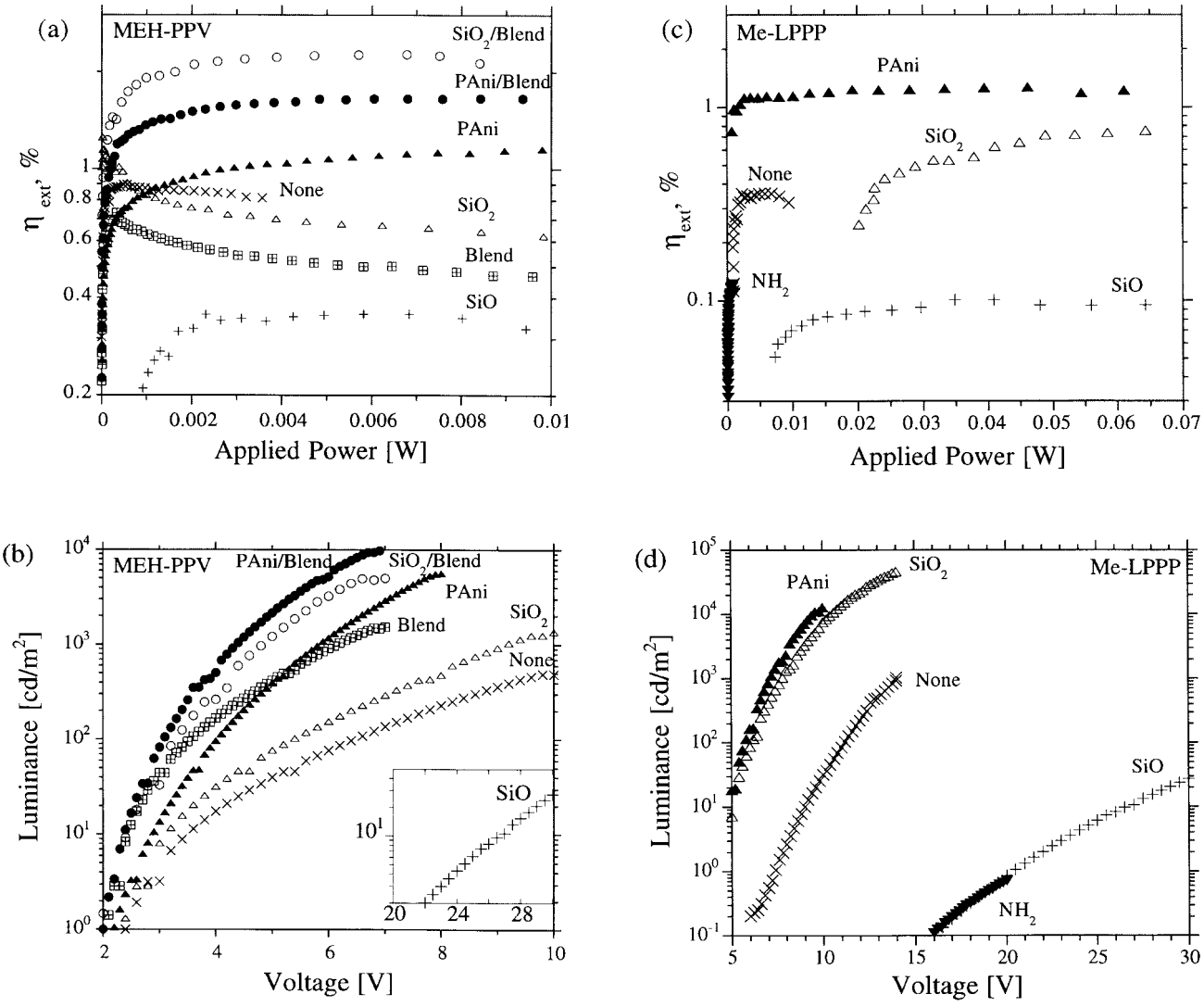

Fig. 2. The external quantum efficiency (a,c) and luminance (b,d) versus applied power and voltage for MEH-PPV- (a,b) and Me-LPPP- (c,d) based polymer light-emitting diodes with Ca cathode and different modifications of the ITO electrode: open symbols are monolayers formed with 20 nm SiO_2 nanoparticles, closed symbols are 100 nm PAni thin films, pluses are for 20 nm SiO thin films and crosses are for no modification (bare ITO). The circles and crossed squares contain blended active layers (MEH-PPV and SiO_2 nanoparticles). A maximum quantum efficiency near 2.5 % and 1.0 % is achieved using monolayers of SiO_2 nanoparticles for the MEH-PPV- and Me-LPPP-based polymer light-emitting diodes, respectively.

temperatures.[19] The NH_2 modified ITO substrates and devices with the self-assembled polystyrene latex spheres do not lead to any improvement over the unmodified ITO surface. The Au nanoparticle monolayers have much worse performance due to quenching at the metal electrode surface.[20] Luminances (cd/m^2) for the same set of devices are shown in Figure 2b. Greater than one order of magnitude increase in brightness can be obtained using blended structures, as shown previously;[19] however, nanoparticle monolayers themselves do not improve brightness over PAni-based samples, indicating that the monolayers affect injection rather than bulk transport properties.

Similar results for the Me-LPPP active polymer are shown in Figure 2c and 2d. Self-assembly of the SiO_2 nanoparticles or spinning of PAni can give up to two orders of magnitude increase in light output in comparison to the unmodified ITO anode. Quantum efficiencies above 1 % at voltages below 8 V are achieved by improving hole injection; these results are significantly better than previously reported power efficiencies for this material.[13,14] Nanoparticle/Me-LPPP blends do not enhance luminance, as observed for MEH-PPV, due to phase separation that occurs between the Me-LPPP and nanoparticles; the rigid chemical structure of Me-LPPP, and related polyfluorenes, does not contain any dipolar binding sites for the oxide-based nanoparticles. A summary of the quantum efficiency and luminance results for the different nanoparticle modifications are presented in Table 2.

Several possible mechanisms can be used to describe the effect that the SiO_2 nanoparticle monolayer has on the performance of polymer light-emitting diodes. The lack of any improvement when similar sized nanoparticles are used,

  0935-9648/99/1510-1259 $ 17.50+.50/0

Table 2. External quantum efficiencies [%] and luminances [cd/m^2] for the MEH-PPV- and Me-LPPP-based polymer light-emitting diodes for different nanoparticle monolayer modifications of the ITO anode.

Nanoparticles	maximum η_{ext} [%]		luminance [cd/m^2]	
	MEH-PPV	Me-LPPP	MEH-PPV (at 9 V)	Me-LPPP (at 9 V)
SiO_2; 20 nm	2.5	~ 1.3	5000–12000	~ 5000
Au; 40 nm	0.001	0.0005	~ 3	~ 4
PS Latex; 30 nm	0.3	0.2	~ 150	~ 60
none	0.8–1.0	~ 0.4	100	~ 50

such as polystyrene spheres, eliminates geometrical effects, such as decreasing mobility or increasing outcoupling efficiency through scattering. We further note that the outcoupling efficiency is already maximized for the planar polymer geometry (waveguiding occurs preferentially in the glass); the nanoparticles could only serve to reduce the planar geometry by enhancing surface roughness and therefore reduce the outcoupling efficiency *C*. These considerations imply that the nature of the nanoparticle surface, and not its geometry, is of primary importance for the manifestation of the improvement.

The nanoparticle surface can enhance the probability for electron–hole recombination by decreasing the carrier mobility or by providing a preferential site for recombination, or they can aide charge balance through modification of hole injection or electron transport through the structure. The recombination efficiency *b* is increased due to either an increase in the fraction of charges that recombine or an improvement in the balance of injected electrons and holes.

First, we consider that the nanoparticle surface can increase the fraction of charges that recombine (*b* in Eq. 1) by either giving the electrons and holes a favorable site to recombine or giving the carriers time to find each other by reducing their mobility. Clear evidence for charge trapping–detrapping at the nanoparticle surface is observed in all monolayer samples through a hysteresis or charging effect. This trapping–detrapping effectively reduces the carrier mobility which has been suggested to increase the quantum efficiency.[21] For ohmic injection, such a reduction in the mobility would result in a decrease in the current density; however, we observe an increase in the current density with SiO_2 monolayers, not a reduction.

The nanoparticle interface can also serve as a favorable sight for recombination since the SiO_2 surface has been demonstrated to trap both electrons and holes.[22] This effect would increase the quantum efficiency but would not significantly affect the current density. Furthermore, previous results on blends have shown that charge trapping on the surface of SiO_2 nanoparticles reduces the quantum efficiency at low current densities.[19] Therefore, we can not attribute the enhancement in quantum efficiency to a bulk effect.

Alternatively, we can consider that the nanoparticle monolayer increases the recombination efficiency *b* by modifying the density of injected charges or the charge balance inside the bulk. The SiO_2 nanoparticle monolayer surface can contain a net negative charge due to incomplete compensation with the positive charges on the amine group. This net negative charge can either increase the density of electrons in the bulk by providing a barrier for electrons to reach the anode or it can increase the density of injected holes by increasing the electric field across the anode interface, as depicted in Figure 3. The electron blocking properties of silicon oxide were tested using an SiO thermally evaporated thin film of the same thickness as the SiO_2 nanoparticle's diameter (20 nm). As shown in Figure 2, both the quantum efficiency and brightness of such a device were worse in comparison to the nanoparticle device. The NH_2 terminated self-assembled monolayer itself appears to be an effective blocking layer. We observed a reduction of both quantum efficiency and brightness for both NH_2 terminated SAM (self-assembling monolayer) and for vacuum-evaporated SiO layer in devices with any type of active polymer. In addition, these devices have much higher "turn-on" voltage. Therefore, we can conclude that the mechanism of quantum efficiency enhancement is not simply connected to blocking properties.

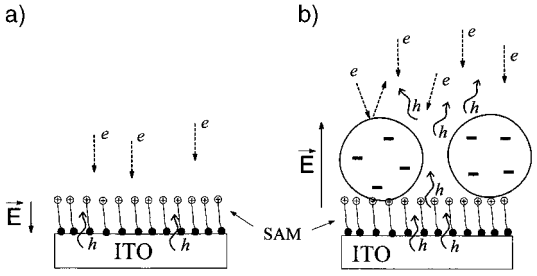

Fig. 3. Diagram showing how self-assembly of the NH_2-terminated alkoxysilane molecules affects the electric field at the ITO interface. Electrostatic assembly of negatively charged nanoparticles onto the self-assembled monolayer results in a reversal of the electric field at this interface. This electrostatic layer can either improve hole injection into the polymer films or serve as an electron blocking layer.

The importance of local field effect can be seen both from the reduction of the quantum efficiency and brightness with an application of an only 9 Å thick layer of charged molecules (NH_2-terminated SAM). Deposition of SiO_2 nanoparticles monolayer reverses the local field across the device, or dipole moment, across the interface, as shown in Figure 3. The effect of this electric field is to increase the hole injection. The increase in both quantum efficiency, brightness and current density, as observed in Figure 2, can therefore be explained if the recombination efficiency *b* is limited by hole-injection. Although most conjugated polymers are considered to be electron-limited, MEH-PPV has previously been shown to be hole-limited when ITO and Ca are used as contacts.[21] This effect is due to the ohmic nature of the Ca electrode whose work function of 2.9 eV is within a tenth of an electron volt from MEH-PPV's lowest unoccupied molecular orbital (LUMO) (~3.0 ± 0.1 eV). Conversely, the ITO electrode, whose work function is 4.8 eV, has a much higher mismatch with respect to the HOMO of MEH-PPV (~5.2 ± 0.1 eV). Therefore, an increase in hole injection can

  0935-9648/99/1510-1260 $ 17.50+.50/0

ADVANCED MATERIALS

result in an improvement in device performance, revealing that Me-LPPP, in addition to MEH-PPV, is hole-limited with a Ca cathode. For conjugated polymer films, such as PAni, the improvement in quantum efficiency is due to an increase in the anode work function to 5.1 ± 0.1 eV, which results in a nearly ohmic contact. For nanoparticle monolayers, the improvement is due to an increase in the local electric field across the interface. This accelerating local electric field is induced by a net negative charge on the nanoparticle surface which results either from silicon hydroxyl groups on the SiO_2 surface or from electrons which are trapped at the interface between the conjugated polymer and nanoparticle.

In conclusion, we have shown that modification of the ITO electrode with SiO_2 nanoparticles can dramatically improve electroluminescence properties of polymer light-emitting devices (PLED). The charged nanoparticle surface, which serves as a carrier trap at low current densities, can induce a dipole moment across the electrode interface, effectively increasing the local electric field and promoting carrier injection. This effect enables the ability to improve PLED efficiency with a single monolayer without including additional polymer layers or modifying the electrode work function. Understanding the nature of the nanoparticle surface will clearly be critical to controlling and optimizing the performance of polymer/nanoparticle composite materials, offering further promise for innovative optoelectronic applications.

Received: January 4, 1999
Final version: June 30, 1999

[1] N. Herron, D. L. Thorn, *Adv. Mater*. **1998**, *10*, 1173.
[2] R. Biswas, M. M. Sigalas, G. Subramania, K.-M. Ho, *Phys. Rev. B* **1998**, *57*, 3701.
[3] F. Hide, B. J. Schwarz, M. A. Diaz-Garcia, A. J. Heeger, *Chem. Phys. Lett.* **1996**, *256*, 424.
[4] B. O'Reagan, M. Gratzel, *Nature* **1991**, *353*, 737.
[5] A. C. Aragno, S. A. Carer, P. J. Brock, *Appl. Phys. Lett.* **1999**, *74*, 1698.
[6] S. A. Carter, J. C. Scott, P. J. Brock, *Appl. Phys. Lett.* **1997**, *71*, 1145.
[7] J. H. Burroughs, D. D. C. Bradley, A. R. Brown, R. N. Marks, K. Makkay, R. H. Friend, P. L. Burns, A. B. Holmes, *Nature* **1990**, *347*, 539.
[8] I. D. Parker, Q. Pei, M. Marrocco, *Appl. Phys. Lett.* **1994**, *65*, 1272.
[9] S. Tanak, C. Adachi, T. Koyama, Y. Taniguchi, *Chem. Lett.* **1998**, *10*, 975.
[10] X. T. Tao, Y. D. Zhang, T. Wada, H. Sasabe, *Appl. Phys. Lett.* **1997**, *71*, 1921.
[11] F. Nuessch, L. Si-Ahmed, B. Francois, L. Zuppiroli, *Adv. Mater.* **1997**, *9*, 222.
[12] P. K. H. Ho, M. Granstrom, R. H. Friend, N. C. Greenham, *Adv. Mater.* **1998**, *10*, 769.
[13] V. V. Tsukruk, V. N. Bliznyuk, *Langmuir* **1998**, *14*, 446.
[14] J. Gruner, P. J. Hamer, R. H. Friend, H.-J. Huber, U. Scherf, A. B. Holmes, *Adv. Mater.* **1994**, *6*, 748.
[15] S. Tasch, A. Niko, G. Leising, U. Scherf, *Appl. Phys. Lett.* **1996**, *68*, 1090.
[16] S. A. Carter, M. Angelopoulos, S. Karg, P. J. Brock, J. C. Scott, *Appl. Phys. Lett.* **1997**, *70*, 2067.
[17] M. Yang, L. J. Rothberg, E. W. Kwock, T. M. Miller, *Phys. Rev. Lett.* **1995**, *75*, 1992.
[18] N. C. Greenham, I. D. W. Samuel, G. R. Heyes, R. T. Phillips, Y. A. R. R. Kessener, S. C. Moratti, A. B. Holmes, R. H. Friend, *Chem. Phys. Lett.* **1995**, *241*, 89. J. C. de Mello, H. F. Wittmann, R. H. Friend, *Adv. Mater.* **1997**, *9*, 230.
[19] L. Bozano, S. E. Tuttle, S. A. Carter, P. J. Brock, *Appl. Phys. Lett.* **1998**, *73*, 3911.
[20] V. E. Choong, T. Park, Y. L. Gao, B. R. Hsieh, *Macromol. Symp.* **1998**, *125*, 83.
[21] G. G. Malliaras, J. R. Salem, P. J. Brock, J. C. Scott, *Phys. Rev. B* **1998**, *58*, R13 411.
[22] A. Yokozawa, Y. Miyamoto, *Appl. Phys. Lett.* **1998**, *73*, 1122.

Ordered Macroporous Materials by Colloidal Assembly: A Possible Route to Photonic Bandgap Materials**

By *G. Subramanian*, *Vinothan N. Manoharan*, *James D. Thorne*, and *David J. Pine**

Ordered macroporous materials with pore sizes in the sub-micrometer range have elicited much interest recently because of their applications in separations processes, catalysis, low dielectric constant materials, and lightweight structural materials. Macroporous oxides such as silica, titania, and zirconia as well as polymers such as polyacrylamide and polyurethane with well-defined pore sizes in the sub-micrometer regime have been successfully synthesized.[1–8] Apart from uses in structural and catalytic materials, the length scales of the pores confer these materials with unique optical properties. For instance, ordered macropores in a high refractive index matrix such as titania can be used to make photonic crystals with a photonic bandgap (PBG).[9] Applications of PBG materials include omnidirectional mirrors, waveguides, and suppression or enhancement of spontaneous emission.[9]

The key to making PBG materials is the requirement to make an ordered dielectric lattice of materials with a high refractive index contrast, n_2/n_1, where n_2 and n_1 refer to the larger and smaller refractive indices in the structure. The minimum contrast required depends on the lattice type and varies from 2.1 for a diamond lattice to about 3 for a face centered cubic (fcc) lattice.[9] Since n_1 cannot be less than 1, the highest refractive index contrast can be obtained by using a high refractive index material with an ordered array of voids. The range of wavelengths over which a crystal exhibits a stop band or omnidirectional bandgap is determined by the lattice spacing of the voids. Thus, to achieve a PBG in the visible, lattice spacings comparable to the wavelength of light are required.

A promising approach to the fabrication of PBG materials with stop bands at visible wavelengths involves the use of self-assembled templates. For synthesis of macroporous materials with pores in the sub-micrometer range, ordered

[*] Dr. D. J. Pine, Dr. G. Subramanian
Materials Department, University of California
Santa Barbara, CA 93106 (USA)
Dr. D. J. Pine, Dr. V. N. Manoharan, Dr. J. D. Thorne
Chemical Engineering Department, University of California
Santa Barbara, CA 93106 (USA)

[**] This research was supported by US Army Grant No. DAAG559710372 and NSF Grant No. 9871970. We gratefully acknowledge useful discussions with F. Lange.

  0935-9648/99/1510-1261 $ 17.50+.50/0